

Geophysical Research Letters

RESEARCH LETTER

10.1029/2020GL087465

Special Section:

The Arctic: An AGU Joint Special Collection

Key Points:

- Unlike previous assumptions, carbon flux attenuation can both be weak and strong in cold Arctic waters (<4 °C)
- Phytoplankton community composition is a more reliable predictor of carbon flux attenuation than temperature alone
- Phytoplankton and zooplankton abundance and composition should be included in carbon flux models as these parameters can modify b

Supporting Information:

- Supporting Information S1
- Table S1

Correspondence to:

I. Wiedmann,
ingrid.wiedmann@uit.no

Citation:

Wiedmann, I., Ceballos-Romero, E., Villa-Alfageme, M., Renner, A. H. H., Dybwad, C., van der Jagt, H., et al. (2020). Arctic observations identify phytoplankton community composition as driver of carbon flux attenuation. *Geophysical Research Letters*, 47, e2020GL087465. <https://doi.org/10.1029/2020GL087465>

Received 17 FEB 2020












Accepted 13 JUN 2020

Accepted article online 24 JUN 2020

©2020. The Authors.

This is an open access article under the terms of the Creative Commons Attribution License, which permits use, distribution and reproduction in any medium, provided the original work is properly cited.

Arctic Observations Identify Phytoplankton Community Composition as Driver of Carbon Flux Attenuation

I. Wiedmann¹ , E. Ceballos-Romero² , M. Villa-Alfageme² , A. H. H. Renner³ , C. Dybwad¹ , H. van der Jagt^{4,5}, C. Svensen¹ , P. Assmy⁶ , J. M. Wiktor⁷ , A. Tatarek⁷ , M. Różańska-Pluta⁷ , and M. H. Iversen⁴ 

¹UiT The Arctic University of Norway, Tromsø, Norway, ²Departamento de Física Aplicada II, Universidad de Sevilla, Spain, ³Institute of Marine Research, Fram Centre, Tromsø, Norway, ⁴Alfred-Wegener-Institute, Helmholtz Center for Polar and Marine Research, Bremerhaven, Germany, ⁵Bureau Waardenburg, Culemborg, Netherlands, ⁶Norwegian Polar Institute, Fram Centre, Tromsø, Norway, ⁷Institute of Oceanology, Polish Academy of Sciences (IOPAN), Sopot, Poland

Abstract The attenuation coefficient b is one of the most common ways to describe how strong the carbon flux is attenuated throughout the water column. Therefore, b is an essential input variable in many carbon flux and climate models. Marsay et al. (2015, <https://doi.org/10.1073/pnas.1415311112>) proposed that the median surface water temperature (0–500 m) may be a predictor of b , but our observations from Arctic waters challenge this hypothesis. We found a highly variable attenuation coefficient ($b = 0.43$ – 1.84) in cold Arctic waters (<4.1 °C). Accordingly, we suggest that water temperature is not a globally valid predictor of the attenuation coefficient. We advocate instead that the phytoplankton composition and especially the relative abundance of diatoms can be used to parametrize the carbon flux attenuation in local and global carbon flux models.

Plain Language Summary In the surface ocean, microalgae convert dissolved atmospheric CO₂ into organic carbon (OC). As OC sinks in the water column, microbes and zooplankton graze on it. It has been suggested that these organisms reduce the amount of sinking OC stronger in warm waters than in cold waters. We found, however, that the amount of sinking OC is sometimes strongly and sometimes weakly reduced in cold Arctic waters (<4 °C). Therefore, we conclude that temperature seems not to be an important factor determining how strong the amount of sinking OC is reduced with depth. We instead advocate that the phytoplankton community composition is useful to predict how strong the amount of sinking OC is reduced with depth. When fast-sinking algae form algal aggregates or are repackaged into copepod fecal pellets, their OC spends only a short time in the upper water column where hungry grazers are very abundant. The consumers have then much less time to prey on the OC than when the sinking particles consist of slowly sinking algae. Concluding, we argue that it is very important to include the phytoplankton community composition in computer simulations to correctly predict how much OC is stored in the oceans.

1. Introduction

In a global perspective, today's oceans act as a carbon sink, exporting carbon from the euphotic zone to depth through the biological carbon pump or other multifaceted modes of export (Boyd et al., 2019). However, only 10% of the sinking carbon reaches depth below 500 m (Wassmann et al., 2003) because organic carbon is utilized by microbes and zooplankton in the upper water column. Quantifying the carbon flux attenuation by these heterotrophs is key for global carbon flux models, because only then these models can estimate the ocean's ability to act as carbon sink at present and in the future. Implementing regulating processes into carbon flux models is however not straightforward because both the sinking velocity (w) and the remineralization (k) of carbon changes with depth (z). A recent compilation by Cael and Bisson (2018) presents seven different parameterizations of the vertical carbon flux attenuation depending on w and k . However, the most common method to estimate the carbon flux attenuation is still the power law function by Martin et al. (1987):

$$F_z = F_{z_0} (z/z_0)^{-b} \quad (1)$$

The attenuation coefficient b characterizes here the shape of the vertical carbon flux between a shallow reference depth z_0 with the carbon flux F_{z_0} and a carbon flux F_z at greater depth z (Equation 1).

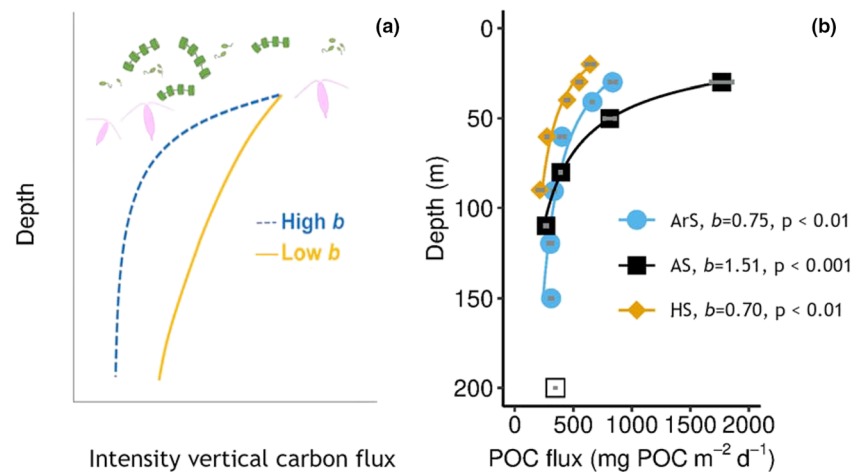


Figure 1. (a) Conceptual illustration of the carbon flux attenuation in the upper water column. Blue stippled line illustrates a strong carbon attenuation (with a high attenuation coefficient b) and the orange line a weak carbon attenuation (with a low attenuation coefficient b). (b) Vertical flux of carbon at station HS (Hornsund Station, orange diamonds), ArS (Arctic Station, blue filled circles), and Atlantic Station (AS, black squares) with the standard deviation of the estimated flux (gray bars) and nonlinear least squares fits (colors corresponding to the colors used for the stations). Residual standard errors for the fits are presented in Table S1. The open square indicates data that have not been used to estimate the attenuation coefficient b by the nonlinear square fit, because the sediment trap cylinder at 190 m was most likely exposed to advected water masses (as suggested by the somewhat enhanced chlorophyll a concentrations between 150 and 200 m at station AS; Figure 2c).

Martin et al. (1987) suggested that an attenuation coefficient of $b = 0.858$ would be globally valid, even though their field observations showed that b considerably varied regionally and seasonally ($b = 0.648\text{--}0.973$) in the northeast Pacific. This variability has been confirmed by later studies (Henson et al., 2012), but a definite driver of b has still not been identified. Biological drivers such as the phytoplankton community composition (Guidi et al., 2009, 2015) or the particle composition and ballasting (Iversen & Ploug, 2010; Ploug, Iversen, & Fischer, 2008; Ploug, Iversen, Koski, et al., 2008) have been suggested to determine the sinking velocity of carbon and thus affect b . However, even though there is increasing evidence that models incorporating ecological processes perform better (Estapa et al., 2019), detailed biological information is often scant and difficult to implement into large scale models. An easily obtained driver of b , such as latitude, would therefore be preferred, but the conclusions drawn for latitude have even been opposing (Buesseler et al., 2007, vs. Henson et al., 2012, Marsay et al., 2015). Marsay et al. (2015) alternatively proposed water temperature as a driver of b , because warm water regions appeared to be characterized by a high b , while a low b seemed to be representative of cold-water regions (Figure 1a). As higher temperatures result in higher growth and respiration rates of heterotrophic bacteria (Iversen & Ploug, 2013; Kirchman et al., 2009), higher bacterial remineralization rates in warmer than colder waters seem reasonable. However, the study by Marsay et al. (2015) only included observations from tropical, temperate, and subpolar regions ($>4^\circ\text{C}$) in the Northern Hemisphere. As the Arctic Ocean is an important carbon sink (Stein & Macdonald, 2004), it is essential to implement the carbon cycling in these areas correctly into global carbon flux models. Therefore, we test here the hypothesis that the correlation between temperature and attenuation coefficient b is also valid in cold, Arctic systems.

2. Materials and Methods

2.1. Field Sampling and Sample Analyses

During the ARCEX cruise with R/V *Helmer Hanssen* in May 2016, three stations around Svalbard were investigated (Figure S1 and Table S2 in the supporting information). Station Hornsund (HS, $77^\circ01.002'\text{N}$, $16^\circ28.408'\text{E}$) was located in the semienclosed Hornsund on the western coast of Svalbard. It was characterized by largely open water with a few drifting sea ice floes during our fieldwork (ice concentration: $<10\%$). The Arctic Station (ArS, $79^\circ10.079'\text{N}$, $26^\circ22.163'\text{E}$), located east of Svalbard in the Erik Eriksen Strait between Nordaustlandet and Kongsøya, was mainly influenced by Arctic-derived waters and was covered

with drift ice (concentration: 40%). The Atlantic Station (AS) was located in ice-free waters of the western Barents Sea (76°13.352'N, 29°38.115'E) and influenced by Atlantic-derived waters.

At each station, hydrographic data were collected using a Seabird CTD SBE 911plus, equipped with temperature (SBE 3plus), conductivity (SBE 4C), and fluorescence (Seapoint fluorometer) sensors. Raw CTD data were preprocessed using SBE processing software. Final processing and calibration of the conductivity sensor against salinity samples was done using a suite of Matlab routines for despiking, removal of wakes, extracting the downcast, and deriving 1 db-binned profiles. A constant offset was applied for salinity correction. Water samples were collected from 7 to 8 depths between 0 m and 120 m using a Niskin rosette (Table S2). Triplicated subsamples of 100–200 ml were filtered onto Whatman GF/F filters (pore size 0.7 μm) for chlorophyll *a* (Chl *a*) concentrations and 200–300 ml were filtered onto precombusted GF/F filters for particulate organic carbon (POC) analyses. In the present work, we use the term carbon to refer to POC and neglect a potential impact of dissolved organic carbon. Chl *a* samples were frozen ($-20\text{ }^{\circ}\text{C}$) and analyzed within 2 months after filtration using the acidification method (Holm-Hansen & Riemann, 1978). Data obtained with the CTD fluorometer were calibrated against these Chl *a* concentrations. POC samples were analyzed on a Leeman Lab CEC 440 CHN Analyzer (procedures following Reigstad et al., 2008). In addition, 100 ml subsamples were collected for enumeration and taxonomy determination of phytoplankton (fixed with 1 ml glutaraldehyde-lugol solution) under inverted microscopes (Nikon Ti-S and Te300, magnification 100, 200, and 600X) following the Utermöhl method (Edler & Elbrächter, 2010). Zooplankton were collected with a WP-2 net at HS, and a multinet at ArS and AS (details see Table S2) and counted under a stereomicroscope. Raw data were then integrated over the sampled depth interval (Table S2). Short-term sediment traps (KC Denmark, inner diameter 72 mm, height: 450 mm) were deployed for 20–23 hr at each station (Table S2). The sediment trap array was anchored at HS due to limited space for drifting but was free drifting (surface tethered) at ArS and AS. Sinking biomass was collected in the paired sediment trap cylinders at 5–6 sampling depths between 20 and 190 m (Table S2). During sediment trap deployment, CTD profiles were taken in a grid pattern around the anchored or drifting sediment trap array to investigate the spatial variability of temperature, salinity, and fluorescence (Figure S1 and Table S2). After recovery of the sediment traps, the content of the cylinders was transferred to carboys, and subsamples were taken to determine the flux of phytoplankton (100 ml, fixed with 2 ml of glutaraldehyde-lugol solution), Chl *a* (filtration of 50–200 ml), and POC (filtration of 100–300 ml), which were analyzed as described for suspended samples above.

2.2. Attenuation Coefficient b

The attenuation coefficient b was determined at each station (Table S1) between the depth of the highest observed carbon flux (upper limit, Table S1) and the carbon flux at the deepest observation available (lower limit, Table S1). These depth limits were chosen to exclude single instances (e.g., TT07_12N), where the carbon flux in the uppermost trap (50 m) was lower than in the second trap (75 m), because we could then not exclude that the uppermost trap was possibly deployed in the lower euphotic zone and therefore characterized by a lower flux (Wassmann et al., 2003). Further, at station AS, the elevated Chl *a* concentration between 160 and 200 m suggested that this depth was affected by advection (Figure 2c), and we excluded the data from the deepest trap (Figure 1b). The attenuation coefficient b has been approximated by a non-linear least squares fit in RStudio, presuming a Power Law shaped decline of the carbon flux (Martin et al., 1987; see Equation 1). As most of the carbon fluxes were determined by only one deployment of a sediment trap array or a neutrally buoyant sediment trap, direct uncertainties due to advection or lateral transport of carbon could not be obtained. Further, we cannot exclude that the different depth horizon of the sediment trap deployments included in this compilation of different observational studies (uppermost trap at 20–150 m, lowermost at 90–748 m) may influence b in a similar way as the depth horizon has been identified to affect the e -ratio (ratio of carbon flux to net primary production; Palevsky & Doney, 2018). This needs to be taken into consideration when interpreting the results. Finally, all Arctic studies presented here used surface-tethered sediment traps, while Marsay et al. (2015) reported the carbon flux determined by neutrally buoyant sediment traps. As it has been shown that the carbon flux estimated by these two trap types are comparable (Buesseler et al., 2000; Owens et al., 2013), we consider it acceptable to compile data collected with both types of traps.

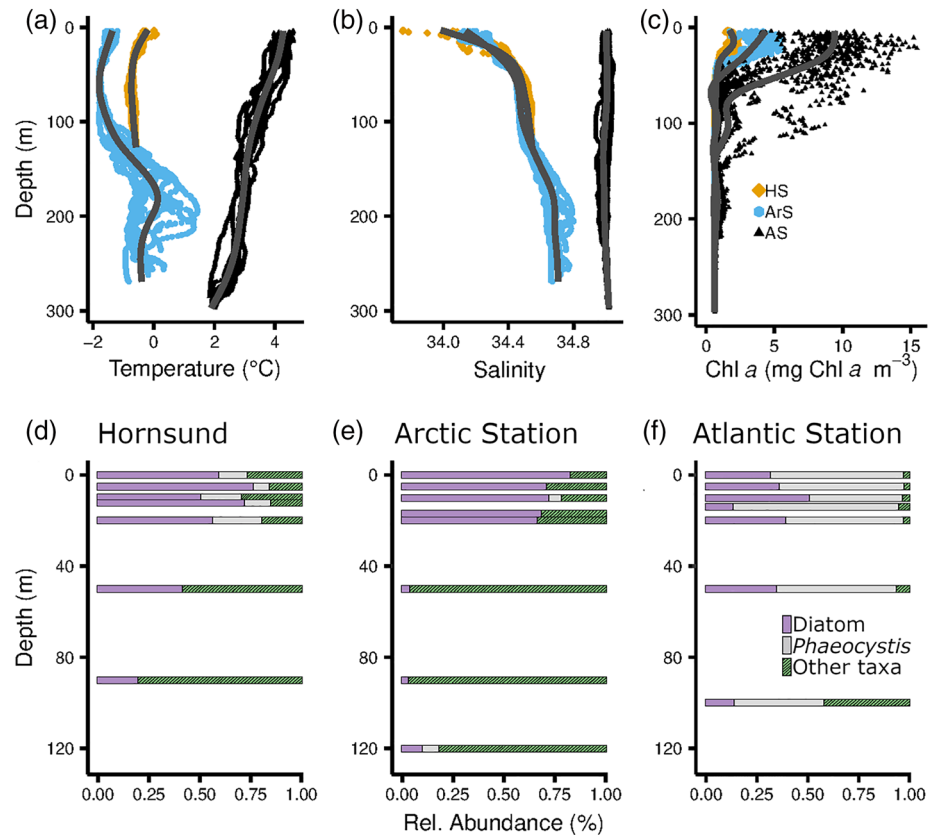


Figure 2. Hydrographical data and chlorophyll *a* (Chl *a*) concentration at the three sampling stations in the upper panel: (a) temperature, (b) salinity, (c) Chl *a* at the Hornsund Station (orange diamonds), the Arctic Station (blue dots), and the Atlantic Station (black triangles). Lower panel shows the relative phytoplankton composition in the water column at the (d) Hornsund Station, (e) the Arctic Station, and (f) the Atlantic Station (purple = diatoms, light gray = *Phaeocystis pouchetii*, shaded green = other taxa).

2.3. Literature Data and Figures

The data compiled here originate from field studies concurrently investigating hydrography, phytoplankton composition and abundance, and vertical carbon flux. Raw data from supplementary information were used whenever possible but extracted from published figures using the WebDigitizer (<https://automeris.io/WebPlotDigitizer/>) when data were not otherwise available. In Table S1, we present the median water temperature of the interval 0–100 m because temperature data from this depth were available for all studies. Principally, only studies assessing the phytoplankton community composition microscopically were included, because it has been shown that data obtained by microscopical inspection and, for example, CHEMTAX are not directly comparable (Armbrecht et al., 2015). However, the stations T4, St35, and St37 were so clearly dominated by one phytoplankton taxon, that we included them even if their community composition was assessed by HPLC and CHEMTAX (Table S1). Further, information on phytoplankton composition was often limited to the most common groups, and we chose to only investigate the correlation between *b* and the relative diatom abundance here, because diatoms are often regarded as fast-sinking phytoplankton (Ploug, Iversen, Koski, et al., 2008). Other ballasted phytoplankton taxa may however also regulate *b*.

3. Results and Discussion

We conducted fieldwork at three stations in the cold waters around the Svalbard archipelago (Figure S1 and Table S2). Water masses in the Arctic-influenced waters at HS and at ArS were characterized by very low temperatures (−1.79 °C to −0.3 °C; Figures S1 and 2a), while the waters at AS (Figure S1) were slightly

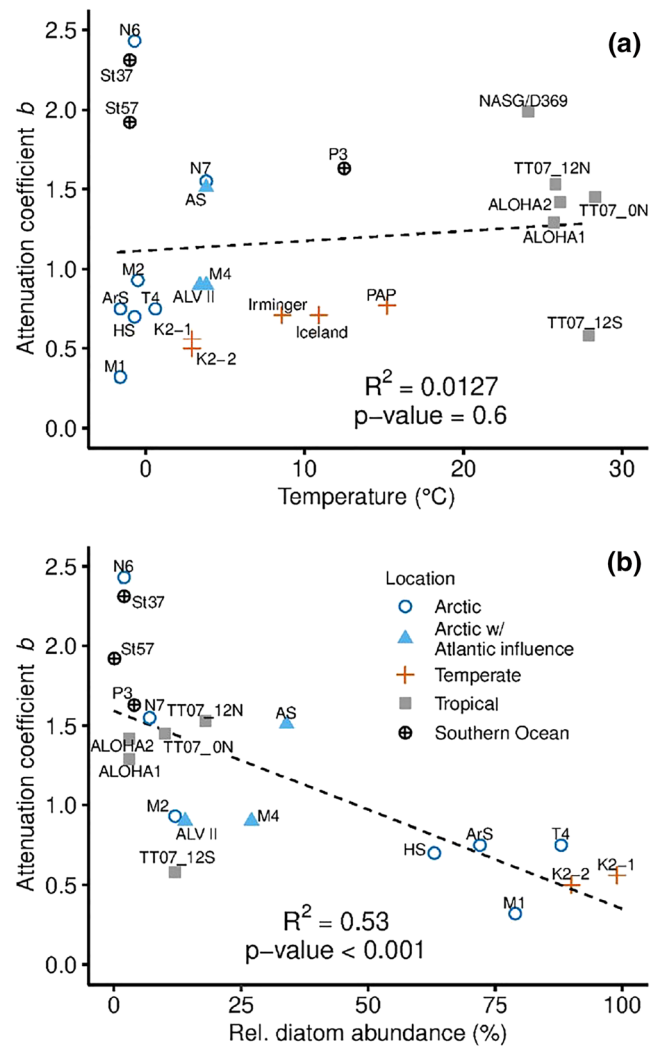


Figure 3. (a) Scatterplot of temperature versus attenuation coefficient *b* compiling data from Marsay et al. (2015) and additional stations (Table S1). (b) Scatterplot of the relative diatom abundance (in % of the total number of suspended microphytoplankton cells) versus attenuation coefficient *b*. Arctic data are symbolized by blue circles, Arctic data with Atlantic influence by blue triangles, temperate data by orange crosses, tropical data by gray squares, and data from the Southern Ocean by black round symbols. Abbreviations refer to the following studies (latitudinal order from north to south): HS, ArS, AS: Present study; M1, M2, M4: Wiedmann et al. (2014); N6, N7: Assmy et al. (2017), Dodd et al. (2016); T4: Dybwad et al. (2020), Nikolopoulos et al. (2016), Peeken (2020); ALVII: Olli et al. (2002), Reigstad et al. (2002), Wassmann et al. (2006); Irminger: BODC (British Oceanography Data Centre, <https://www.bodc.ac.uk>, cruise D354), Marsay et al. (2015); Iceland: BODC (cruise D354), Marsay et al. (2015); PAP: BODC (cruise D341), Marsay et al. (2015); K2-1, K2-2: Marsay et al. (2015), Siegel (2006a, 2006b), Silver (2009); NASG/D369: BODC (cruise 369), Marsay et al. (2015); ALOHA1, 2: Marsay et al. (2015), Pasulka et al. (2013), Siegel (2005a, 2005b); TT07_12N: Fryxell (2003a), Murray and Gardner (2003a), Newton and Murray (2003a); TT07_0N: Fryxell (2003b), Murray and Gardner (2003b), Newton and Murray (2003b), TT07_12S: Fryxell (2003c), Murray and Gardner (2003c), Newton and Murray (2003c), P3: BODC (cruise AU0703), Ebersbach et al. (2011), Petrou et al. (2011), St35/St37: Randall-Goodwin et al. (2015), Yager et al. (2016).

warmer (+2.4 to +4.1 °C; Figure 2a). Salinity was also marginally higher at station AS than at HS and ArS (AS: 34.94–35.01; HS and ArS: 34.1–34.7; Figure 2b), indicative of warmer and more saline Atlantic water masses.

Water temperatures at our three stations were lower than at the ones obtained by Marsay et al. (2015) and, thus, useful to test if the correlation between temperature and the carbon flux attenuation coefficient *b* is valid in the Arctic. Compared to HS, ArS, and previous studies in the area, the downward carbon flux at AS was very high at 30 m (AS: 1768 mg C m⁻² day⁻¹, HS and ArS: 550–830 mg C m⁻² day⁻¹, central

Barents Sea: 200–1,500 mg C m⁻² day⁻¹; Olli et al., 2002; Reigstad et al., 2008) but comparable below 80 m (HS and ArS: 216–333 mg C m⁻² day⁻¹, AS: 266 mg C m⁻² day⁻¹, Figure 1b). We estimated from these data an attenuation coefficient b of 0.70 at station HS and 0.75 at ArS (Figure 1b and Table S1). The b at station AS was, compared to HS and ArS, considerably higher ($b = 1.51$; Figure 1b).

Bringing together the carbon attenuation coefficients from our study with those reported in Marsay et al. (2015; Table S1), other Arctic studies (ALV, CONFLUX, N-ICE2015, and TRANSSIZ; Table S1), data from the Southern Ocean (P3, St35, and St57; Table S1), and the equatorial Pacific (EqPac; Table S1) allows examining the correlation between b and water temperature ranging from -1.7 to $+28.6$ °C (Figure 3a). This extended data set clearly illustrates that b varies over the whole temperature range (Figure 3a), and the low coefficient of determination ($R^2 = 0.01$) suggests a weak correlation between temperature and b . A weak correlation was also found (1) when using the mean or median temperature between uppermost and lowermost sediment trap (Figure S2) instead of the median temperature 0–100 m and (2) between the remineralization length scale and the median temperature (as used in Marsay et al., 2015; Figure S3). This raises the question why a strong correlation ($R^2 > 0.8$) between temperature and b was found by Marsay et al. (2015) but not here. Our data set is larger, and as b is affected by the variable depth range sampled (uppermost trap: 20–150 m, deepest trap: 90–748 m), the number of sampling depths per station (3–10), and the distance to the euphotic zone (Buesseler et al., 2020; Olli, 2015), a weaker correlation may be expected in the present study than in Marsay et al. (2015), because our data set has a generally higher variability.

We speculate however that our weaker correlation is not only caused by differences in field data collection, but that Marsay et al. (2015) also identified the strong correlation because all their field observations were collected in summer. We presume that the pelagic ecosystem functioning in their studies was therefore more comparable and that temperature was likely the only substantially varying parameter at the investigated temperate and tropical sites. From experiments, it is known that temperature has an effect on microbial degradation of settling aggregates, because aggregates have been found to degrade faster at 15 °C than at 4 °C (Iversen & Ploug, 2013). We accordingly speculate that the correlation between the carbon attenuation and temperature identified in Marsay et al. (2015) is only true in instances of similar plankton composition. Then, temperature-dependent microbial remineralization may be the main driver of b . In our extended data set, including both spring and summer observations (i.e., spring bloom and post bloom scenarios), we could not identify a clear correlation between temperature and b (Figure 3a). This suggests that temperature is not the sole predictor of the attenuation coefficient.

Instead, we propose that the seasonal changes in phytoplankton and zooplankton community composition have a major impact on b . During our fieldwork around Svalbard, we encountered three contrasting situations of a peak- to late-spring bloom phase. The Chl a concentration in the subsurface maximum (SCM) was lowest at station HS (SCM at 5 m, 3.34 mg Chl a m⁻³; Figure 2c), intermediate at ArS (SCM at 20 m, 8.25 mg Chl a m⁻³), and highest at AS (no clear SCM; 8–35 m: 4.0–15.5 mg Chl a m⁻³; Figure 2c). The spatial variation of the Chl a concentration was considerably lower at HS and ArS than at AS (Figure 2c), but this potentially resulted from the wider sampling grid around the drifting or anchored sediment trap array (HS and ArS: up to 4 km distance and AS: up to 12 km). The most pronounced difference between the three stations was nevertheless the phytoplankton composition. Waters at station HS and ArS were diatom dominated in the upper 90 to 100 m (HS: 51%–76% of the suspended microalgae cells were diatoms, ArS: 66%–82% diatoms; dominant taxa at both stations: *Thalassiosira* spp., *Fragilariopsis* spp., *Porosira glacialis*; Figures 2d and 2e). Station AS was in contrast dominated by *Phaeocystis pouchetii* (44%–81% of the suspended microalgae cells, 0–100 m; Figure 2f). We hypothesize that the contrasting phytoplankton composition may be a good predictor of the carbon flux attenuation because (1) the taxa dominating in the water column tended also to be frequently found in the exported material (Table S3) and (2) the diatom-dominated waters at HS and ArS were characterized by a low b , while the *P. pouchetii* dominated waters at AS were characterized by a high b (Table S1). This hypothesis of the relative diatom abundance being a driver of b seems to be further supported by the correlation between the relative diatom abundance and the attenuation coefficient reported from the Arctic, temperate and tropical regions, and the Southern Ocean ($R^2 = 0.53$; Figure 3b). However, data from the Southern Ocean are biased because only data with low relative diatom abundances were available. Previous work supports these findings,

because diatoms ballasted with silica frustules tend to sink faster than nonballasted, flagellated phytoplankton taxa (Hansen et al., 1996; Osinga et al., 1996; Reigstad & Wassmann, 2007). It can therefore be speculated that diatom aggregates sink faster than aggregates of nonballasted nanoplankton and spend a shorter time in the “pelagic mill” of the upper water column (Wassmann et al., 2003), where organic carbon is strongly remineralized by microbes and grazed by zooplankton. We therefore argue that fast-sinking diatom aggregates and their carbon content are less likely to be attenuated in the water column. Furthermore, the carbon flux attenuation is also governed by (1) the specific daily cell lysis rate, which is lower for diatoms ($<10\% \text{ day}^{-1}$) than flagellates ($<33\% \text{ day}^{-1}$; Brussaard et al., 1996) and (2) the fact that copepod fecal pellets produced from a diatom diet sink faster and withstand microbial breakdown better than pellets produced from a flagellate diet (Hansen et al., 1996; Ploug, Iversen, Koski, et al., 2008; Thor et al., 2003). Accordingly, we advocate that the carbon flux attenuation tends not to be defined by water temperature alone, but b is rather controlled by a combination of temperature-regulated microbial remineralization and the prevailing phytoplankton community.

Interestingly, previous studies have also proposed a correlation between the predominant phytoplankton size class and b , but they suggested the exactly opposite relation (microphytoplankton dominance characterized by a high b , picoplankton systems by a low b ; Guidi et al., 2009, 2015). We can only speculate if the different approaches caused this difference (present study: microscopically determined phytoplankton data, carbon flux determined by sediment traps; Guidi et al., 2009: phytoplankton size classes estimated by HPLC, carbon flux calculated from particle abundances obtained by an Underwater Video Profiler). Nevertheless, we hypothesize, in congruence with Guidi et al. (2009), that zooplankton can play a role determining b .

The interplay between zooplankton and b is illustrated for example by our observations at stations AS and M4. Both stations were located in the western Barents Sea (median temperature 0–100 m: $3.8 \text{ }^\circ\text{C}$; Table S1). Though the phytoplankton community at both stations was characterized by a high relative abundance of *P. pouchetii*, b was considerably different (AS: $b = 1.51$, M4: $b = 0.9$). We speculate that this difference in b was caused by the tenfold higher copepod abundance at M4 (0–100 m: AS: $43,600 \text{ ind. m}^{-2}$ vs. M4: $500,000 \text{ ind. m}^{-2}$). The abundant copepods at M4 seem to have converted many of the slowly sinking algae (sinking velocity of *P. pouchetii* colonies: 10 m day^{-1} ; Ploug et al., 1999) into faster sinking fecal pellets (sinking velocity of *Calanus finmarchicus* pellets: $20\text{--} > 100 \text{ m day}^{-1}$; Urban-Rich et al., 1999), because fecal pellets were the dominant vehicle of export observed in sediment traps modified with a gel-containing glass jar at 40 and 60 m (Figure S4). At station AS, where the Chl *a* concentration was much higher (AS: $6.5 \mu\text{g Chl } a \text{ L}^{-1}$; M4: $0.9 \mu\text{g Chl } a \text{ L}^{-1}$; Figure 2c; Wiedmann et al., 2014) but the copepod abundance considerably lower than at M4, and more phytoaggregates were exported at 40 m (Figure S4). We presume that these phytoaggregates had a low sinking velocity because they probably consisted mainly of the dominant, slowly sinking phytoplankton species *P. pouchetii*. Accordingly, we speculate that zooplankton affected b , because it converted the slowly sinking phytoplankton cells and phytoaggregates into fast-sinking pellets. In this form, carbon was more resistant against remineralization and could “escape” remineralization in the upper water column through fast sinking, and contribute to a lower b at M4.

Overall, we show based on our extended data set (median water temperature 0–100 m: <0 to $28 \text{ }^\circ\text{C}$) that water temperature alone seems not to be a reliable predictor of the carbon flux attenuation coefficient b . Instead, we suggest that the composition of phytoplankton (i.e., ballasted and fast-sinking vs. not-ballasted and slowly sinking taxa) can be a central driver of the carbon flux attenuation. The more (less) ballasted and sticky phytoplankton (e.g., diatoms; Kiørboe & Hansen, 1993) that are present in the upper water column, the higher (lower) the probability is for the formation of fast sinking aggregates and ballasted fecal pellets, which are exposed for a shorter (longer) period to temperature-dependent microbial degradation and zooplankton grazing in the upper water column. This, in turn, results in a weaker (stronger) carbon flux attenuation. Based on these findings, we recommend that global carbon flux models based on the Martin equation (Martin et al., 1987) should not parameterize b solely by water temperature but take the relative abundance of ballasted phytoplankton (e.g., diatoms, coccolithophores) into account. This is in accordance with recent findings that export models including ecosystem parameters perform better (Estapa et al., 2019).

Acknowledgments

We thank the captain and the crew of the R/V Helmer Hanssen for help in the field, Paul Wassmann, Allison Fong, Rolf Gradinger, and the attendees of the Biarritz Workshop for their fruitful discussions, Marit Reigstad, Kalle Olli, Sharon Stammerjohn, and Evan Randall-Goodwin for insight into old data, and Helena Kling Michelsen and Nicole Hildebrandt for the zooplankton analyses. Further, we greatly appreciated the constructive comments of two anonymous reviewers. This work contains data supplied by the Natural Environment Research Council (UK) and the open data platform of the JGOFS and the VERTIGO programs, whose PIs allowed us to use their data in this work. We also thank the team of the free WebPlotDigitizer (<https://automeris.io/WebPlotDigitizer/>) and the publication fund of UiT The Arctic University of Norway. All new data can be found in the UiT Open Research Data archive (<https://doi.org/10.18710/GSMVQY>). This work and IW's contribution was funded by ARCEX, the Research Centre for Arctic Petroleum Exploration (Research Council of Norway, #228107) and industry partners. P.A. was funded by the Research Council of Norway (#244646 and #268286), the Ministry of Foreign Affairs, Norway (project ID Arctic), and the former Centre for Ice, Climate, and Ecosystems (ICE) at the Norwegian Polar Institute. J.W., A.T., and M.R.P. were financially supported by the -add comma before & Polish Ministry of Science and Higher Education (grant W6/Norway/2017).

References

Armbrrecht, L. H., Wright, S. W., Petocz, P., & Armand, L. K. (2015). A new approach to testing the agreement of two phytoplankton quantification techniques: Microscopy and CHEMTAX. *Limnology and Oceanography: Methods*, *13*(8), 425–437. <https://doi.org/10.1002/lom3.10037>

Assmy, P., Fernández-Méndez, M., Duarte, P., Meyer, A., Randelhoff, A., Mundy, C. J., et al. (2017). Leads in Arctic pack ice enable early phytoplankton blooms below snow-covered sea ice. *Scientific Reports*, *7*, 40850. <https://doi.org/10.1038/srep40850>

Boyd, P. W., Claustre, H., Levy, M., Siegel, D. A., & Weber, T. (2019). Multi-faceted particle pumps drive carbon sequestration in the ocean. *Nature*, *568*(7752), 327–335. <https://doi.org/10.1038/s41586-019-1098-2>

Brussaard, C. P. D., Gast, G. J., van Duyl, F. C., & Riegman, R. (1996). Impact of phytoplankton bloom magnitude on a pelagic microbial food web. *Marine Ecology Progress Series*, *144*, 211–221. <https://doi.org/10.3354/meps144211>

Buesseler, K. O., Boyd, P. W., Black, E. E., & Siegel, D. A. (2020). Metrics that matter for assessing the ocean biological carbon pump. *Proceedings of the National Academy of Sciences*, *117*(18), 9679–9687. <https://doi.org/10.1073/pnas.1918114117>

Buesseler, K. O., Lamborg, C. H., Boyd, P. W., Lam, P. J., Trull, T. W., Bidigare, R. R., et al. (2007). Revisiting carbon flux through the ocean's twilight zone. *Science*, *316*(5824), 567–570. <https://doi.org/10.1126/science.1137959>

Buesseler, K. O., Steinberg, D. K., Michaels, A. F., Johnson, R. J., Andrews, J. E., Valdes, J. R., & Price, J. F. (2000). A comparison of the quantity and composition of material caught in a neutrally buoyant versus surface-tethered sediment trap. *Deep Sea Research Part I: Oceanographic Research Papers*, *47*(2), 277–294. [https://doi.org/10.1016/S0967-0637\(99\)00056-4](https://doi.org/10.1016/S0967-0637(99)00056-4)

Cael, B. B., & Bisson, K. (2018). Particle flux parameterizations: Quantitative and mechanistic similarities and differences. *Frontiers in Marine Science*, *5*, 395. <https://doi.org/10.3389/fmars.2018.00395>

Dodd, P., Meyer, A., Koenig, Z., Cooper, A., Smedsrud, L. H., Muilwijk, M., et al. (2016). N-ICE2015 ship-based conductivity-temperature-depth (CTD) data [data set]. Norwegian Polar Institute. <https://doi.org/10.21334/npolar.2017.92262a9c>

Dybwad, C., Reigstad, M., Nikolopoulos, A., Peeken, I., Kristiansen, S. (2020). Concentrations of suspended and exported organic matter and nutrients during POLARSTERN cruise PS92 (ARK-XXIX/1 TRANSSIZ) in May and June 2015 north of Svalbard. UiT The Arctic University of Norway, PANGAEA, <https://doi.org/10.1594/PANGAEA.910883>

Ebersbach, F., Trull, T. W., Davies, D. M., & Bray, S. G. (2011). Controls on mesopelagic particle fluxes in the Sub-Antarctic and Polar Frontal Zones in the Southern Ocean south of Australia in summer - Perspectives from free-drifting sediment traps. *Deep Sea Research II*, *58*, 2260–2276. <https://doi.org/10.1016/j.dsr2.2011.05.025>

Edler, L., & Elbrächter, M. (2010). The Utermöhl method for quantitative phytoplankton analysis. In B. Karlson, C. Cusack, & E. Bresnan (Eds.), *Microscopic and Molecular Methods for Quantitative Phytoplankton Analysis*, (pp. 13–20). Paris: UNESCO.

Estapa, M. L., Feen, M. L., & Breves, E. (2019). Direct observations of biological carbon export from profiling floats in the subtropical North Atlantic. *Global Biogeochemical Cycles*, *33*, 282–300. <https://doi.org/10.1029/2018GB006098>

Fryxell, G. A. (2003a). Abundance and carbon biomass of phytoplankton at station TT007_1-CTD14. PANGAEA. (Data set accessed on 12.06.2019). <https://doi.org/10.1594/PANGAEA.122734>

Fryxell, G. A. (2003b). Abundance and carbon biomass of phytoplankton at station TT007_8-CTD102. PANGAEA. (Data set accessed on 12.06.2019). <https://doi.org/10.1594/PANGAEA.122745>

Fryxell, G. A. (2003c). Abundance and carbon biomass of phytoplankton at station TT007_15-CTD162. PANGAEA. (Data set accessed on 13.6.2019). <https://doi.org/10.1594/PANGAEA.122738>

Guidi, L., Legendre, L., Reygondeau, G., Uitz, J., Stemmann, L., & Henson, S. A. (2015). A new look at ocean carbon remineralization for estimating deepwater sequestration. *Global Biogeochemical Cycles*, *29*, 1044–1059. <https://doi.org/10.1002/2014gb005063>

Guidi, L., Stemmann, L., Jackson, G. A., Ibanez, F., Claustre, H., Legendre, L., et al. (2009). Effects of phytoplankton community on production, size, and export of large aggregates: A world-ocean analysis. *Limnology and Oceanography*, *54*(6), 1951–1963. <https://doi.org/10.4319/lo.2009.54.6.1951>

Hansen, B., Fotel, F. L., Jensen, N. J., & Madsen, S. D. (1996). Bacteria associated with a marine planktonic copepod in culture. II. Degradation of fecal pellets produced on a diatom, a nanoflagellate or a dinoflagellate diet. *Journal of Plankton Research*, *18*(2), 275–288. <https://doi.org/10.1093/plankt/18.2.275>

Henson, S. A., Sanders, R., & Madsen, E. (2012). Global patterns in efficiency of particulate organic carbon export and transfer to the deep ocean. *Global Biogeochemical Cycles*, *26*, GB1028. <https://doi.org/10.1029/2011gb004099>

Holm-Hansen, O., & Riemann, B. (1978). Chlorophyll *a* determination: Improvements in methodology. *Oikos*, *30*(3), 438–447. <https://doi.org/10.2307/3543338>

Iversen, M. H., & Ploug, H. (2010). Ballast minerals and the sinking carbon flux in the ocean: carbon-specific respiration rates and sinking velocity of marine snow aggregates. *Biogeosciences*, *7*, 2613–2624. <https://doi.org/10.5194/bg-7-2613-2010>

Iversen, M. H., & Ploug, H. (2013). Temperature effects on carbon-specific respiration rate and sinking velocity of diatom aggregates-potential implications for deep ocean export processes. *Biogeosciences*, *10*(6), 4073–4085. <https://doi.org/10.5194/bg-10-4073-2013>

Kjørboe, T., & Hansen, J. L. S. (1993). Phytoplankton aggregate formation: Observations of patterns and mechanisms of cell sticking and the significance of exopolymeric material. *Journal of Plankton Research*, *15*(9), 993–1018. <https://doi.org/10.1093/plankt/15.9.993>

Kirchman, D. L., Morán, X. A. G., & Ducklow, H. (2009). Microbial growth in the polar oceans—Role of temperature and potential impact of climate change. *Nature Reviews Microbiology*, *7*(6), 451–459. <https://doi.org/10.1038/nrmicro2115>

Marsay, C. M., Sanders, R. J., Henson, S. A., Pabortsava, K., Achterberg, E. P., & Lampitt, R. S. (2015). Attenuation of sinking particulate organic carbon flux through the mesopelagic ocean. *Proceedings of the National Academy of Sciences*, *112*(4), 1089–1094. <https://doi.org/10.1073/pnas.1415311112>

Martin, J. H., Knauer, G. A., Karl, D. M., & Broenkow, W. W. (1987). VERTEX: Carbon cycling in the northeast Pacific. *Deep Sea Research Part A. Oceanographic Research Papers*, *34*(2), 267–285. [https://doi.org/10.1016/0198-0149\(87\)90086-0](https://doi.org/10.1016/0198-0149(87)90086-0)

Murray, J. W., & Gardner, W. (2003a). Physical oceanography at station TT007_1-CTD14. PANGAEA. (Data set accessed on 13.6.2019). <https://doi.org/10.1594/PANGAEA.119816>

Murray, J. W., & Gardner, W. (2003b). Physical oceanography at station TT007_8-CTD102. PANGAEA. (Data set accessed on 13.6.2019). <https://doi.org/10.1594/PANGAEA.119949>

Murray, J. W., & Gardner, W. (2003c). Physical oceanography at station TT007_15-CTD150. PANGAEA. (Data set accessed on 13.6.2019). <https://doi.org/10.1594/PANGAEA.119858>

Newton, J., & Murray, J. W. (2003a). Particulate carbon, nitrogen and chlorophyll pigments of sediment trap TT007_1-HTR1. PANGAEA. (Data set accessed on 12.06.2019). <https://doi.org/10.1594/PANGAEA.125558>

- Newton, J., & Murray, J. W. (2003b). Particulate carbon, nitrogen and chlorophyll pigments of sediment trap TT007_9-Murray_trap. PANGAEA. (Data set accessed on 12.06.2019). <https://doi.org/10.1594/PANGAEA.125567>
- Newton, J., & Murray, J. W. (2003c). Particulate carbon, nitrogen and chlorophyll pigments of sediment trap TT007_15-Murray_trap. PANGAEA. (Data set accessed on 12.06.2019). <https://doi.org/10.1594/PANGAEA.125561>
- Nikolopoulos, A., Janout, M., Hölemann, J. A., Juhls, B., Korhonen, M., & Randelhoff, A. (2016). Physical oceanography during POLARSTERN cruise PS92 (ARK-XXIX/1). Alfred Wegener Institute, Helmholtz Centre for Polar and Marine Research, Bremerhaven, PANGAEA, <https://doi.org/10.1594/PANGAEA.861865>
- Olli, K. (2015). Unraveling the uncertainty and error propagation in the vertical flux Martin curve. *Progress in Oceanography*, 135, 146–155. <https://doi.org/10.1016/j.pocean.2015.05.016>
- Olli, K., Riser, C. W., Wassmann, P., Ratkova, T., Arashkevich, E., & Pasternak, A. (2002). Seasonal variation in vertical flux of biogenic matter in the marginal ice zone and the central Barents Sea. *Journal of Marine Systems*, 38(1-2), 189–204. [https://doi.org/10.1016/S0924-7963\(02\)00177-X](https://doi.org/10.1016/S0924-7963(02)00177-X)
- Osinga, R., Kwint, R. L. J., Lewis, W. E., Kraay, G. W., Lont, J. D., Lindeboom, H. J., & van Duyl, F. (1996). Production and fate of dimethylsulfide and dimethylsulfoniopropionate in pelagic mesocosms: The role of sedimentation. *Marine Ecology Progress Series*, 131, 275–286. <https://doi.org/10.3354/meps131275>
- Owens, S. A., Buesseler, K. O., Lamborg, C. H., Valdes, J., Lomas, M. W., Johnson, R. J., et al. (2013). A new time series of particle export from neutrally buoyant sediments traps at the Bermuda Atlantic Time-series Study site. *Deep Sea Research Part I: Oceanographic Research Papers*, 72, 34–47. <https://doi.org/10.1016/j.dsr.2012.10.011>
- Palevsky, H. I., & Doney, S. C. (2018). How choice of depth horizon influences the estimated spatial patterns and global magnitude of ocean carbon export flux. *Geophysical Research Letters*, 45, 4171–4179. <https://doi.org/10.1029/2017GL076498>
- Pasulka, A. L., Landry, M. R., Taniguchi, D. A. A., Taylor, A. G., & Church, M. J. (2013). Temporal dynamics of phytoplankton and heterotrophic protists at station ALOHA. *Deep Sea Research Part II: Topical Studies in Oceanography*, 93, 44–57. <https://doi.org/10.1016/j.dsr2.2013.01.007>
- Peeken, I. (2020). Chemtax based phytoplankton group composition during POLARSTERN cruise PS92. PANGAEA, <https://doi.org/10.1594/PANGAEA.917802>
- Petrou, K., Hassler, C. S., Doblin, M. A., Shelly, K., Schoemann, V., van den Enden, R., et al. (2011). Iron-limitation and high light stress on phytoplankton populations from the Australian Sub-Antarctic Zone (SAZ). *Deep Sea Research Part II: Topical Studies in Oceanography*, 58, 2200–2200. <https://doi.org/10.1016/j.dsr2.2011.05.020>
- Ploug, H., Iversen, M. H., & Fischer, G. (2008). Ballast, sinking velocity, and apparent diffusivity within marine snow and zooplankton fecal pellets: Implications for substrate turnover by attached bacteria. *Limnology and Oceanography*, 53(5), 1878–1886. <https://doi.org/10.4319/lo.2008.53.5.1878>
- Ploug, H., Iversen, M. H., Koski, M., & Buitenhuis, E. T. (2008). Production, oxygen respiration rates, and sinking velocity of copepod fecal pellets: Direct measurements of ballasting by opal and calcite. *Limnology and Oceanography*, 53(2), 469–476. <https://doi.org/10.4319/lo.2008.53.2.0469>
- Ploug, H., Stolte, W., Epping, E. H. G., & Jørgensen, B. B. (1999). Diffusive boundary layers, photosynthesis, and respiration of the colony-forming plankton algae, *Phaeocystis* sp. *Limnology and Oceanography*, 44(8), 1949–1958. <https://doi.org/10.4319/lo.1999.44.8.1949>
- Randall-Goodwin, E., Meredith, M. P., Jenkins, A., Yager, P. L., Sherrell, R. M., Abrahamsen, E. P., et al. (2015). Freshwater distributions and water mass structure in the Amundsen Sea Polynya region, Antarctica. *Elementa: Science of the Anthropocene*, 3, 000065. <https://doi.org/10.12952/journal.elementa.000065>
- Reigstad, M., Riser, C. W., Wassmann, P., & Ratkova, T. (2008). Vertical export of particulate organic carbon: Attenuation, composition and loss rates in the northern Barents Sea. *Deep Sea Research Part II: Topical Studies in Oceanography*, 55(20-21), 2308–2319. <https://doi.org/10.1016/j.dsr2.2008.05.007>
- Reigstad, M., & Wassmann, P. (2007). Does *Phaeocystis* spp. contribute significantly to vertical export of organic carbon? *Biogeochemistry*, 83(1–3), 217–234. <https://doi.org/10.1007/s10533-007-9093-3>
- Reigstad, M., Wassmann, P., Riser, C. W., Øygarden, S., & Rey, F. (2002). Variations in hydrography, nutrients and chlorophyll a in the marginal ice-zone and the central Barents Sea. *Journal of Marine Systems*, 38(1–2), 9–29. [https://doi.org/10.1016/S0924-7963\(02\)00167-7](https://doi.org/10.1016/S0924-7963(02)00167-7)
- Siegel, D. A. (2005a). CTD station profile data, program: VERTIGO, cruise: KM0414, platform: R/V kilo Moana, 25.06.2004. (Data set accessed on 11.06.2019). http://ocb.whoi.edu/jg/serv/OCB/VERTIGO/KM0414/ctd.html?date_HST%20eq%2020040625
- Siegel, D. A. (2005b). CTD station profile data, program: VERTIGO, cruise: KM0414, platform: R/V kilo Moana, 07.05.2004. (Data set accessed on 23.04.2020). http://ocb.whoi.edu/jg/serv/OCB/VERTIGO/KM0414/ctd.html?Bdir=ocb.whoi.edu/jg/dir/OCB/VERTIGO/KM0414/info=ocb.whoi.edu:80/jg/info/OCB/VERTIGO/KM0414/ctd%7D?date_HST%20eq%2020040705
- Siegel D. A. (2006a). CTD station profile data, program: VERTIGO, cruise: RR_K2, platform: R/V Revelle, 31.07.2005. (Data set accessed on 23.04.2020). http://ocb.whoi.edu/jg/serv/OCB/VERTIGO/RR_K2/ctd.html?Bdir=ocb.whoi.edu/jg/dir/OCB/VERTIGO/RR_K2/info=ocb.whoi.edu:80/jg/info/OCB/VERTIGO/RR_K2/ctd%7D?cast%20eq%2019
- Siegel D. A. (2006b). CTD station profile data, program: VERTIGO, cruise: RR_K2, platform: R/V Revelle, 10.08.2005. (Data set accessed on 23.04.2020). http://ocb.whoi.edu/jg/serv/OCB/VERTIGO/RR_K2/ctd.html?Bdir=ocb.whoi.edu/jg/dir/OCB/VERTIGO/RR_K2/info=ocb.whoi.edu:80/jg/info/OCB/VERTIGO/RR_K2/ctd%7D?cast%20eq%2063
- Silver, M. W. (2009). Phytoplankton species data and biomass data: abundance and fluxes from CTDs from VERTIGO cruises KM0414, NW SubArctic Pacific Ocean K2 Site, 2004–2005, VERTIGO project. (Data set accessed on 25.10.2019). http://ocb.whoi.edu/jg/serv/OCB/VERTIGO/RR_K2/phytobio_CTD.html?Bdir=ocb.whoi.edu/jg/dir/OCB/VERTIGO/RR_K2/info=ocb.whoi.edu:80/jg/info/OCB/VERTIGO/RR_K2/phytobio_CTD%7D?ev_code%20eq%20CTD_018
- Stein, R., & Macdonald, R. W. (2004). Organic carbon budget: Arctic Ocean vs. global ocean. In R. Stein, & R. W. Macdonald (Eds.), *The Organic Carbon Cycle in the Arctic Ocean* (pp. 315–322). Berlin, Heidelberg: Springer. https://doi.org/10.1007/978-3-642-18912-8_8
- Thor, P., Dam, H. G., & Rogers, D. R. (2003). Fate of organic carbon released from decomposing copepod fecal pellets in relation to bacterial production and ectoenzymatic activity. *Aquatic Microbial Ecology*, 33(3), 279–288. <https://doi.org/10.3354/ame033279>
- Urban-Rich, J., Nordby, E., Andreassen, I., Wassmann, P., & Høisæter, T. (1999). Contribution by mezooplankton focal pellets to the carbon flux on Nordvestkbanken, north Norwegian shelf in 1994. *Sarsia*, 84, 253–264. <https://doi.org/10.1080/00364827.1999.10420430>
- Wassmann, P., Olli, K., Riser, C. W., & Svensen, C. (2003). Ecosystem function, biodiversity and vertical flux regulation in the twilight zone. In G. Wefer, F. Lamy, & F. Mantoura (Eds.), *Marine Science Frontiers for Europe* (pp. 279–287). Berlin, Heidelberg: Springer.

- Wassmann, P., Slagstad, D., Riser, C. W., & Reigstad, M. (2006). Modelling the ecosystem dynamics of the Barents Sea including the marginal ice zone: II. Carbon flux and interannual variability. *Journal of Marine Systems*, 59(1–2), 1–24. <https://doi.org/10.1016/j.jmarsys.2005.05.006>
- Wiedmann, I., Reigstad, M., Sundfjord, A., & Basedow, S. (2014). Potential drivers of sinking particle's size spectra and vertical flux of particulate organic carbon (POC): Turbulence, phytoplankton, and zooplankton. *Journal of Geophysical Research: Oceans*, 119, 6900–6917. <https://doi.org/10.1002/2013JC009754>
- Yager, P., Sherrell, R., Stammerjohn, S., Ducklow, H., Schofield, O., Ingall, E., et al. (2016). A carbon budget for the Amundsen Sea Polynya, Antarctica: Estimating net community production and export in a highly productive polar ecosystem. *Elementa: Science of the Anthropocene*, 4, 000140. <http://doi.org/10.12952/journal.elementa.000140>